Ar n HF van der Waals clusters revisited: II. Energetics and HF vibrational frequency shifts from diffusion Monte Carlo calculations on additive and nonadditive potential-energy surfaces for n = 1 - 12

Hao Jiang, Minzhong Xu, Jeremy M. Hutson, and Zlatko Bačić

Articles you may be interested in

Spectroscopy of Ar–SH and Ar–SD. I. Observation of rotation-vibration transitions of a van der Waals mode by double-resonance spectroscopy
J. Chem. Phys. **123**, 054324 (2005); 10.1063/1.1943967

Infrared spectroscopy and structures of Ar n – HF in liquid helium nanodroplets
J. Chem. Phys. **115**, 10138 (2001); 10.1063/1.1392378

Nonadditive intermolecular forces in Ar n –HF van der Waals clusters: Effects on the HF vibrational frequency shift
J. Chem. Phys. **111**, 8378 (1999); 10.1063/1.480179

Time-dependent wave packet study of the one atom cage effect in I 2 –Ar Van der Waals complexes
J. Chem. Phys. **110**, 960 (1999); 10.1063/1.478141

Non-additive intermolecular forces from the spectroscopy of Van der Waals trimers: A comparison of Ar 2 – HF and Ar 2 – HCl , including H/D isotope effects
J. Chem. Phys. **106**, 6288 (1997); 10.1063/1.473645
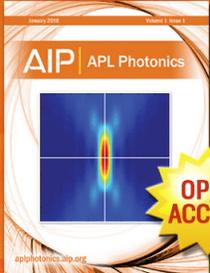
Ar$_n$HF van der Waals clusters revisited: II. Energetics and HF vibrational frequency shifts from diffusion Monte Carlo calculations on additive and nonadditive potential-energy surfaces for *n*=1-12

Hao Jiang and Minzhong Xu
Department of Chemistry, New York University, New York, New York 10003

Jeremy M. Hutson[a]
Department of Chemistry, University of Durham, South Road, Durham, DH1 3LE, United Kingdom

Zlatko Bačić[b]
Department of Chemistry, New York University, New York, New York 10003

The ground-state energies and HF vibrational frequency shifts of Ar$_n$HF clusters have been calculated on the nonadditive potential-energy surfaces (PESs) for *n*=2-7 and on the pairwise-additive PESs for the clusters with *n*=1-12, using the diffusion Monte Carlo (DMC) method. For *n* > 3, the calculations have been performed for the lowest-energy isomer and several higher-lying isomers which are the closest in energy. They provide information about the isomer dependence of the HF redshift, and enable direct comparison with the experimental data recently obtained in helium nanodroplets. The agreement between theory and experiment is excellent, in particular, for the nonadditive DMC redshifts. The relative, incremental redshifts are reproduced accurately even at the lower level of theory, i.e., the DMC and quantum five-dimensional (rigid Ar$_n$) calculations on the pairwise-additive PESs. The nonadditive interactions make a significant contribution to the frequency shift, on the order of 10%–12%, and have to be included in the PESs in order for the theory to yield accurate magnitude of the HF redshift. The energy gaps between the DMC ground states of the cluster isomers are very different from the energy separation of their respective minima on the PES, due to the considerable variations in the intermolecular zero-point energy of different Ar$_n$HF isomers. © *2005 American Institute of Physics.*
[DOI: 10.1063/1.1991856]

I. INTRODUCTION

For nearly 20 years, considerable experimental and theoretical activities have been focused on the Ar$_n$HF clusters, with the goal of advancing our quantitative understanding of intermolecular forces on a microscopic level. The pioneering experimental studies were those of Gutowsky *et al.*[1–3] who used microwave spectroscopy to determine the vibrationally averaged geometries of Ar$_n$HF clusters for *n*=1−4, and of McIlroy *et al.* who measured the vibrational frequency shift (redshift) of the HF fundamental in these clusters[4] and of the DF fundamental in Ar$_n$DF clusters with *n*=1−3.[5]

Motivated by these early size-selected experimental data available for *n* ≤ 4 clusters, Bacic and co-workers set out to develop theoretical methodology which would allow both reproducing from first principles the known spectroscopic properties of small clusters, and accurate prediction of the structures and HF redshifts for various isomers of larger Ar$_n$HF clusters with *n* > 4 not yet observed then. The minimum-energy structures and low-lying isomers of Ar$_n$HF clusters were determined for *n*=1−14, on pairwise-additive potential-energy surfaces (PESs) of very high quality.[6] This

was followed by the quantum five-dimensional (5D) calculations (rigid Ar$_n$), also using pairwise-additive PESs, which predicted the size dependence of the HF redshift in the energetically optimal isomers of Ar$_n$HF clusters for *n* up to 14,[7] as well as the redshifts of several low-energy isomeric structures for each cluster size in this range.[8] In parallel, the HF redshifts were calculated for *n*=1−4 in full dimensionality,[9] using the diffusion Monte Carlo (DMC) method and the pairwise-additive PESs, and on nonadditive PESs by means of the quantum 5D treatment for *n*=2−4, 12.[10]

The above calculations made it clear that the addition of an Ar atom to the first solvation shell around the HF led to a substantial jump of the HF redshift, while adding an argon atom to the second, third, and further solvent shells, not in direct contact with the HF, caused a much smaller increase of the HF redshift.[8] This meant that the redshift would provide a unique spectroscopic signature for the Ar$_n$HF isomers having the same *n* but differing by the number of Ar atoms in the first solvation shell, which could potentially be used in their experimental identification.[8,11]

At the time of the publication of our theoretical studies,[6–10] the chances for their experimental validation were rather slim. The situation changed dramatically with the recent experimental breakthrough of Nauta and Miller,[12] who grew the Ar$_n$HF clusters in the novel, ultracold environment

[a]Electronic mail: j.m.hutson@durham.ac.uk
[b]Author to whom correspondence should be addressed. Electronic mail: zlatko.bacic@nyu.edu

of helium nanodroplets, and measured their infrared (IR) spectra. By changing the order of the pickup of the HF and argon, they managed for the first time to prepare multiple isomers of $n=4-7$ clusters, with HF bound either on the surface or in the interior of the argon microcluster. Nauta and Miller[12] found excellent agreement between the trends in their observed HF redshifts and those predicted by theory,[7–10] which enabled them to assign most of the IR spectra to the isomers calculated by us earlier. Only in two instances, for $n=6, 7$, the assignments were made to the Ar_nHF isomers which were not identified by the calculations. This prompted us to revisit the problem of low-energy isomeric structures in this system, which resulted in the determination of new global minima of the clusters with $n=7, 10, 11$, and new low-lying local minima for these and other cluster sizes up to $n=13$. These results were reported in Ref. 13, which will be referred to as I.

The interaction between theory and experiment on Ar_nHF clusters has been very fruitful, and already provided rather detailed insight into their structures and the IR spectroscopy. But, from the theoretical point of view, an important element was still missing from the comprehensive theoretical description—the DMC calculations of the HF frequency shifts on the nonadditive PESs, for a significant range of cluster sizes. They constitute the most rigorous treatment of the frequency shifts, on the best PESs available. Such calculations are reported for the first time in this paper for $n=2-7$ and several low-lying isomers of each cluster size (for $n>3$). They provide benchmark results against which more approximate theories can be tested, and define the limit of the accuracy with which the frequency shifts in larger rare-gas heteroclusters can be calculated at the present time. Also presented here are the results of the most extensive DMC calculations of the size and isomer dependence of the HF redshifts on the pairwise-additive PESs, for n ranging from 1 to 12, when the first solvation shell is completed.[6] The comparison of these two sets of the DMC calculations with the quantum 5D results obtained previously,[7,8,10] and with the experimental results,[12] provides definitive answers to several important questions: (i) How large is the intermolecular zero-point energy of the Ar_nHF clusters, and how much does it affect the energy gap between the isomers? (ii) What is the effect of the vibrations of the Ar_n microcluster on the HF redshifts? (iii) How significant a contribution do the nonadditive interactions make to the redshifts? (iv) How well do the theory and experiment agree, at different levels of treatment? These and other related issues are discussed in considerable detail.

II. METHODOLOGY

A. Potential-energy surfaces

The potential-energy surfaces used in the present work are constructed from highly accurate pairwise-additive and nonadditive components. The Ar–Ar potential is the HFD–C potential of Aziz and Chen,[14] which was obtained from a multiproperty analysis. The Ar–HF potential is the H6(4,3,2) potential of Hutson,[15] which was fitted to extensive results from high-resolution microwave, far-, and mid-IR

spectroscopy. The pairwise-additive PESs used here are the same as those used in Ref. 6. They depend on the vibrational state of the HF molecule [ground ($v=0$) or excited ($v=1$)] through the parametric dependence of the anisotropic two-dimensional (2D) Ar–HF pair potential on the HF vibrational quantum number v.[15]

Ar_nHX clusters ($X=F$, Cl) are an important testing ground for models of nonadditive intermolecular forces in molecular systems, which are quite different from nonadditive forces between atoms. Cooper and Hutson[16] showed that a major contribution to the nonadditivity in Ar_2HCl arises from the interaction between the permanent dipole and quadrupole of HCl and an exchange quadrupole that is generated when two Ar atoms overlap. They developed a model that included this and showed that it worked well for nonadditive shifts in the far-infrared spectrum of Ar_2HCl. The model was applied to vibrational frequency shifts in Ar_2HF and Ar_2HCl.[17] It was subsequently improved by representing the exchange quadrupole in terms of dipoles on the Ar atoms and introducing cross terms between the exchange and field-induced dipoles[18] and applied to the far-infrared and mid-infrared spectra of Ar_2HF, Ar_2DF, Ar_2HCl, and Ar_2DCl.[18,19] Finally, the model was generalized to handle multiple Ar atoms.[10] The nonadditive potential used in the present DMC calculations is the "total 1" model of Ref. 10, which includes contributions from the nonadditive dispersion, induction, and exchange overlap. The dependence on v is incorporated through the v-dependent multipole moments of HF. It is a many-body model rather than simply a three-body one, since all the contributions to the exchange/induction dipole on each Ar atom are summed before the interaction energy is computed. This model was successfully implemented in the quantum 5D (rigid Ar_n) calculations of the HF frequency shifts.[10]

B. Diffusion Monte Carlo calculations of ground-state energies and HF vibrational frequency shifts

The ground-state properties of quantum many-body systems can be calculated exactly by means of the DMC method. Originally developed by Anderson,[20,21] the DMC method exploits the fact that the time-dependent Schrödinger equation for the imaginary time $\tau=it$ is analogous to the diffusion equation with an additional source/sink term, and can therefore be solved by a random walk. Detailed descriptions of the DMC method are available in the literature.[22–25] Our DMC calculations employ the continuous weighting method[23,24] to keep the number of walkers constant.

On PESs with multiple minima which correspond to different cluster isomers, straightforward DMC simulations will yield the ground state of the lowest-energy isomer. To obtain the ground-state energy of a higher-energy isomer, it is necessary to generate the corresponding wave function such that it is orthogonal to the ground-state wave functions of the lower-energy isomer(s). When the potential barriers separating the higher-energy isomers from those energetically below are high, this can be achieved by initializing all random walkers at the equilibrium configuration of the isomer of interest. In the high-barrier case, there is a negligibly small

a) b) c) d)

n=2   n=3   n=4, i=1   n=4, i=2

e) f) g) h)

n=5, i=1   n=5, i=2   n=5, i=3   n=6, i=1

i) j) k) l)

n=6, i=3   n=6, i=4   n=6, i=7   n=6, i=9

m) n) o) p)

n=7, i=1   n=7, i=2   n=9, i=1   n=12, i=1
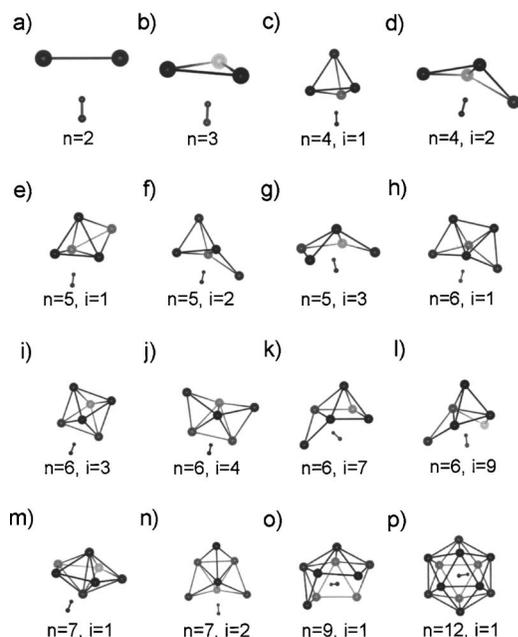
FIG. 1. Selected low-energy isomeric structures of Ar$_n$HF clusters calculated for additive PESs in Refs. 6 and 13.

probability that in the course of the random-walk simulation a walker will be found outside the potential well where it was initiated, and in which the isomer considered resides. Hence, the DMC simulation will converge to the ground state of this isomer without any special effort.

Problems arise if the barriers separating the isomers are low at least along some of the internal coordinates. Then, the probability is nonzero that in the course of a random walk some walkers will escape the potential well in which they were originally placed, into the lower-energy regions of the PES. The weights of such walkers increase rapidly since they are more favored energetically, and they reproduce themselves through branching. As a result, the amplitude of the wave function in the higher-energy potential well will decay quickly to zero and accumulate in one or more lower-energy potential minima, so that the DMC calculation will give the ground-state energy of a lower-lying isomer, not of the higher-energy isomer of interest.

For the clusters such as Ar$_n$HF, the leakage of the wave function out of a higher-energy potential well during the simulation is largely an artifact of the random sampling algorithm of the DMC. As long as the well can support a bound state, the isomer in its ground state will be long lived (on the experimental time scales). Its decay by tunneling through the barrier into the lower-energy minima will be very slow, since it would involve the motion of several heavy argon atoms from one configuration to another. In order to reproduce this physical reality, the standard DMC algorithm has to be modified slightly, so as to prevent the escape of the random walkers from the potential well associated with the particular isomer considered. A characteristic feature of Ar$_n$HF isomers is the number of Ar atoms in the first solvent shell around the HF molecule, denoted as m. For the low-lying isomers, this number is known from their equilibrium structures,[6,13] some of which are shown in Fig. 1. During the

simulation, m can be monitored for each configuration visited by the random walk. If walkers with the value(s) of m different from that of the isomer of interest are detected, they are removed from the ensemble. This procedure ensures that the wave function remains confined within the potential well supporting this isomer. It is similar in spirit to the fixed-node approximation for calculating excited states, with potential barriers playing the role of the nodal surfaces. In the simulations, the value of m for any configuration is obtained by counting the number of Ar atoms which satisfy the condition

$$r_{\mathrm{Ar}_i-\mathrm{HF}} \leqslant \tilde{r}, \tag{1}$$

where $r_{\mathrm{Ar}_i-\mathrm{HF}}$ is the distance between the ith Ar atom and the center of mass of the HF, and the value of $\tilde{r}$ is taken from the DMC calculations of the lowest-energy isomers whose equilibrium structures have more than one solvent shell around the HF. Although empirical, this procedure has proved robust and reliable for calculating the ground-state energies of different Ar$_n$HF isomers.

The HF vibrational frequency shift $\Delta\nu_{n,i}$ of the ith isomer of Ar$_n$HF can be calculated rigorously as the difference between the ground-state energies of this isomer for HF $v=1$ ($E_{n,i}^{v=1}$) and $v=0$ ($E_{n,i}^{v=0}$),[8,9]

$$\Delta\nu_{n,i} = E_{n,i}^{v=1} - E_{n,i}^{v=0}. \tag{2}$$

The ground-state energies $E_{n,i}^{v=0}$ and $E_{n,i}^{v=1}$ are obtained from two separate DMC calculations. In these calculations, the HF bond lengths are held fixed at 0.9220 and 0.9398 Å, respectively, the vibrationally averaged values for the ground and the first excited state of the free HF molecule. This is done using the constraint dynamics method of Sarsa et al.[26] Importance sampling was not employed in the simulations reported here. The DMC calculations used an ensemble of 1000 walkers and the time step of 10 a.u. For each cluster size and isomer considered, the simulations involved 20 independent runs. In every run, after the initial equilibration, the ensemble was propagated in 120 blocks consisting of 1200 steps each.

III. RESULTS AND DISCUSSION

A. The zero-point energy of Ar$_n$HF clusters and its contribution to the energy separation between cluster isomers

Table I gives the intermolecular vibrational ground-state energies of the low-lying isomers of Ar$_n$HF clusters with $n=1-12$, from the DMC calculations on the pairwise-additive and nonadditive PESs, for HF $v=0$ and $v=1$. For a given n, the isomers are labeled with the index i, where $i=1$ designates the lowest-energy isomer and $i>1$ denotes the higher-energy isomeric structures, arranged in the order of increasing energy. Another index which appears in Table I and all subsequent tables is m, which denotes the number of Ar atoms in the first solvation shell of the HF. The ground-state energy decreases steadily with increasing cluster size, indicating that adding an Ar atom enhances the stability of the cluster. Inclusion of the nonadditive interactions in the PES leads to higher ground-state energies. For a given isomer, the ground-state energy, pairwise-additive and nonaddi-

TABLE I. Intermolecular vibrational ground-state energies of the low-lying isomers of Ar$_n$HF clusters, $n=1$ -12, from the DMC calculations on additive (ad.) and nonadditive (nonad.) PESs. $E_{n,i}^{v=0}$ and $E_{n,i}^{v=1}$ are ground-state energies of the ith isomer of the cluster size n, for HF $v=0$ and $v=1$, respectively. The index $i=1$ denotes the lowest-energy isomer, while $i>1$ labels the higher-energy structures, in the order of increasing energies; m is the number of Ar atoms in the first solvation shell of the HF molecule. All energies are in cm^{-1}.

m	n	i	$E_{n,i}^{v=0}$ (ad.)	$E_{n,i}^{v=1}$ (ad.)	$E_{n,i}^{v=0}$ (nonad.)	$E_{n,i}^{v=1}$ (nonad.)
1	1	1	-101.20 ± 0.05	-110.85 ± 0.06		
2	2	1	-284.71 ± 0.07	-300.22 ± 0.07	-276.86 ± 0.08	-291.31 ± 0.09
3	3	1	-553.20 ± 0.09	-573.95 ± 0.09	-529.13 ± 0.08	-547.83 ± 0.09
3	4	1	-817.36 ± 0.11	-838.68 ± 0.11	-781.35 ± 0.11	-800.41 ± 0.11
3	5	1	-1085.42 ± 0.10	-1107.06 ± 0.11	-1039.76 ± 0.09	-1059.06 ± 0.09
3	6	3	-1384.54 ± 0.15	-1406.32 ± 0.15	-1326.33 ± 0.12	-1345.99 ± 0.14
3	6	4	-1361.30 ± 0.17	-1382.97 ± 0.16		
3	7	1	-1720.30 ± 0.14	-1742.47 ± 0.15	-1645.02 ± 0.14	-1664.99 ± 0.16
4	4	2	-816.77 ± 0.11	-840.17 ± 0.11	-779.82 ± 0.10	-801.34 ± 0.11
4	5	2	-1086.40 ± 0.09	-1110.39 ± 0.11	-1037.49 ± 0.10	-1059.19 ± 0.11
4	6	1	-1442.51 ± 0.15	-1467.04 ± 0.15	-1374.23 ± 0.10	-1396.33 ± 0.11
4	7	2	-1718.75 ± 0.17	-1743.56 ± 0.17	-1639.92 ± 0.10	-1662.34 ± 0.14
4	8	1	-2076.82 ± 0.20	-2101.83 ± 0.20		
4	10	3	-2795.60 ± 0.26	-2820.99 ± 0.27		
5	5	3	-1082.80 ± 0.12	-1108.39 ± 0.11	-1034.92 ± 0.12	-1058.56 ± 0.12
5	6	7	-1376.03 ± 0.16	-1401.08 ± 0.16	-1317.09 ± 0.15	-1340.46 ± 0.20
5	6	9	-1356.56 ± 0.18	-1382.56 ± 0.18	-1297.65 ± 0.15	-1321.46 ± 0.17
5	9	2	-2425.91 ± 0.23	-2452.19 ± 0.24		
5	11	2	-3216.15 ± 0.32	-3243.33 ± 0.31		
6	6	2	-1438.52 ± 0.14	-1467.06 ± 0.14	-1372.48 ± 0.14	-1398.57 ± 0.12
6	8	3	-2076.15 ± 0.16	-2105.59 ± 0.17		
6	12	2	-3753.52 ± 0.42	-3784.06 ± 0.44		
9	9	1	-2439.44 ± 0.21	-2475.09 ± 0.23		
10	10	1	-2831.95 ± 0.28	-2868.76 ± 0.26		
11	11	1	-3262.80 ± 0.30	-3301.65 ± 0.31		
12	12	1	-3814.54 ± 0.30	-3855.19 ± 0.30		

tive, calculated for HF $v=1$ is lower than that obtained for HF $v=0$, reflecting of the fact that the strength of the Ar–HF interaction (i.e., the potential-well depth) increases upon vibrational excitation of the HF monomer.

Our previous quantum 5D bound-state calculations for Ar$_n$HF clusters, $n=4-14$,[8] revealed that the energy gap between the ground states of the two lowest-lying isomers (and others as well) of a given cluster size was very different from the energy separation between their respective potential minima. The reason for this is, of course, that Ar$_n$HF isomers differ in their zero-point energies (ZPEs), which affects the energy difference between them. However, the Ar$_n$ moiety is taken to be rigid in the quantum 5D calculations, and therefore they give only the ZPE of the intermolecular vibrations of the HF relative to the frozen Ar$_n$.[8] The ZPE of the Ar$_n$ cluster is not accounted for in this reduced-dimensionality treatment, leaving open the question of its contribution to the isomer energy gap.

This question, and the entire issue of the true energy separation between the Ar$_n$HF isomers, is definitively settled by the DMC calculations in this work, which treat rigorously all intermolecular degrees of freedom of the clusters. The DMC ground-state energies presented in Table I are used to calculate the energy gaps among the low-lying isomers of the $n=4-12$ clusters on the pairwise-additive and (in most cases) nonadditive PESs, for HF $v=0$ and $v=1$, which are shown in Table II. These DMC energy gaps are compared with the energy differences between the corresponding potential minima on the pairwise-additive PESs and, for a few isomers, with the energy gaps from the quantum 5D calculations (rigid Ar$_n$).[8] The energy separations in Table II are mostly those between the lowest-energy isomer ($i=1$) and the next higher isomer ($i=2$); the results shown in the last two lines, for $n=5$, 6, involve the isomers $i=2$ and $i=3$.

It is evident from Table II that the DMC ground-state energy gaps between the two lowest-lying isomers differ very substantially from the energy spacings between their respective potential minima. However, two qualitatively distinct types of differences are observed for $n=4-8$ and 9-12 clusters. For $n=4-8$, the DMC energy gap is invariably *much smaller* than the corresponding potential-energy gap. On the pairwise-additive PESs and for HF $v=0$, the inclusion of the ZPE greatly reduces the energy separation from $\sim13-30$ cm^{-1} between the potential minima to a gap of just $\sim0.5-4$ cm^{-1} between the ground-state energies of the two isomers; for $n=5$, it even reverses the order of the isomers. The same is qualitatively true for the nonadditive PESs as well, although the actual DMC energy gaps have slightly different values. What this means is that for $n=4-8$, on both additive and nonadditive PESs, the ZPE of the minimum-energy ($i=1$) isomer is larger than that of the isomer associated with the next higher ($i=2$) potential minimum, by an amount which is close to the energy difference between the

TABLE II. Energy differences (in cm^{-1}) between the minimum-energy isomer ($i=1$) and the next higher isomer ($i=2$) of Ar$_n$HF clusters, $n=4$-12. For given n, $\Delta V^{v=0}_{2,1}$ (ad.) is the energy difference of the potential minima $V^{v=0}_{n,2}$ and $V^{v=0}_{n,1}$ on the additive PES and HF $v=0$ (Refs. 6 and 13). $\Delta E^{v=0}_{2,1}$ (ad.) and $\Delta E^{v=0}_{2,1}$ (nonad.) are the differences between the DMC ground-state energies $E^{v=0}_{n,2}$ and $E^{v=0}_{n,1}$ of the two isomers, on the additive (ad.) and nonadditive (nonad.) PESs, respectively, for HF $v=0$, given in Table I. $\Delta E^{v=1}_{2,1}$ (ad.) and $\Delta E^{v=1}_{2,1}$ (nonad.) are defined in the same way, but for HF $v=1$. For comparison, $\Delta E^{v=0}_{2,1}$ (Q5D, ad.) are shown in the third column when available, from the quantum 5D calculations on additive PESs in Ref. 8.

n	$\Delta V^{v=0}_{2,1}$ (ad.)	$\Delta E^{v=0}_{2,1}$ (Q5D, ad.)	$\Delta E^{v=0}_{2,1}$ (ad.)	$\Delta E^{v=1}_{2,1}$ (ad.)	$\Delta E^{v=0}_{2,1}$ (nonad.)	$\Delta E^{v=1}_{2,1}$ (nonad.)
4	15.43	5.90	0.59±0.16	−1.49±0.16	1.53±0.15	−0.93±0.16
5	13.42	5.35	−0.98±0.13	−3.33±0.16	2.27±0.13	−0.13±0.14
6	29.26	13.64	3.99±0.20	−0.02±0.21	1.75±0.17	−2.24±0.16
7	16.09		1.55±0.22	−1.09±0.23	5.10±0.17	2.65±0.21
8[a]	23.88	11.14	0.67±0.26	−3.76±0.26		
9	0.24		13.53±0.31	22.9±0.33		
10[b]	3.99		36.35±0.38	47.77±0.37		
11	22.31		46.65±0.44	58.32±0.44		
12	43.32		61.02±0.52	71.13±0.53		
5[c]	15.07	9.20	3.60±0.15	2.00±0.16	2.57±0.16	0.63±0.16
6[c]	17.73		53.98±0.21	60.74±0.21	46.15±0.18	52.58±0.18

[a]For $n=8$, the energy differences shown are between the isomers $i=1$ and $i=3$, since the DMC calculations were not performed for the $i=2$ isomer (Fig. 3 of Ref. 13).
[b]For $n=10$, the energy differences shown are between the isomers $i=1$ and $i=3$, because the geometry of $i=2$ isomer is essentially that of $i=1$, and differs from it only in minor distortions of the Ar$_{10}$ cage. The isomers $i=1$ and $i=3$ are displayed in Fig. 5 of Ref. 13.
[c]The energy differences shown are between the isomers $i=2$ and $i=3$. For $n=5$, the isomers are displayed in Fig. 1, while the $n=6$ isomers are displayed in Fig. 1 of Ref. 13.

two minima. As a result, the two lowest-lying isomers of $n=4-8$ clusters are nearly degenerate. The DMC calculations of Lewerenz[27] for $n=1-4$ clusters produced a similar result for $n=4$.

These ZPE differences can be rationalized by considering the geometries of the isomers in question. The minimum-energy isomers of $n=4-8$ clusters shown in Fig. 1 (for $n=8$, see Fig. 3 in I) have the HF bound to a three- or fourfold surface site of the Ar$_n$ microcluster. In the $i=2$ isomers of $n=4-8$, shown for $n=4$, 5, 7 in Fig. 1 and for $n=6$ and 8 ($i=3$) in I (Figs. 1 and 3), the number of Ar atoms in the first solvation layer around the HF is always greater than in the $i=1$ isomers, making the shell somewhat more open. For this reason, in the $i=2$ isomers the internal motions of the HF are less hindered, and thus have a bit smaller ZPE, than in the $i=1$ isomers of the same cluster size n. Moreover, for the same n, the Ar$_n$ microclusters of the $i=1$ isomers are generally more compact and rigid, and therefore have a higher ZPE, than those of the $i=2$ isomers. That the ZPE of the Ar$_n$ subunits plays a role in determining the energy separation between isomers is evident from the fact the ground-state energy gaps from the quantum 5D calculations (rigid Ar$_n$) for $n=4-6$, 8 shown in Table II are considerably larger than the corresponding DMC energy gaps.

Finally, one can see in Table II that for $n=4-8$, the vibrational excitation of the HF to $v=1$ generally leads to the reversal of the energy ordering of the two lowest-energy isomers, on both additive and nonadditive PESs.

In the case of $n=9-12$ clusters, unlike those with $n=4-8$ above, the energy gap between the DMC ground states of the two lowest-lying isomers is *considerably bigger* than the energy separation of their potential minima. The difference is particularly striking for $n=9$, 10. The implication is in this

range of cluster sizes it is the $i=2$ isomers that have a larger ZPE than the minimum-energy ($i=1$) isomers of the same n. Again, this is readily explained by comparing the equilibrium structures of the isomers in question, shown in Figs. 4–7 in I. The lowest-energy isomers of $n=9$-12 clusters have the HF inside the shell formed by all Ar atoms. The anisotropy of the interaction of the HF with the solvent cage is small, and the motion of the HF is only weakly hindered and therefore has a relatively small ZPE. On the other hand, in the $i=2$ isomers, the HF is in a surface site where it moves on a strongly anisotropic PES, which results in a larger ZPE. Greater rigidity of the polytetrahedral Ar$_n$ structures of the $i=2$ isomers relative to the monolayer cage Ar$_n$ configuration of the $i=1$ isomers also contributes to the greater overall ZPE of the former.

Taken together, these results make it clear that for floppy clusters such as Ar$_n$HF, the energy differences between the global and low-lying local minima on the PESs do not provide an accurate prediction of the true energy gaps between the corresponding cluster isomers, and in some cases of their energy ordering. This can be accomplished only through full-dimensional calculations of the ground-state energies of the isomers, using methods such as the DMC.

B. Size and isomer dependence of Ar$_n$HF vibrational frequency shifts on pairwise-additive and nonadditive potential-energy surfaces

For a given isomer of the Ar$_n$HF cluster considered, the HF vibrational frequency shift can be determined rigorously as the difference between the intermolecular vibrational ground-state energies of this isomer calculated for HF $v=1$ and $v=0$, respectively.[8] The DMC ground-state cluster energies listed in Table I were therefore used to obtain the HF

TABLE III. Calculated and experimental HF vibrational frequency shifts (in cm^{-1}) of the low-energy isomers of Ar$_n$HF clusters. $\Delta\nu_{n,i}$ (DMC, ad.) and $\Delta\nu_{n,i}$ (DMC, nonad.) are the shifts for the ith isomer of Ar$_n$HF, obtained from the DMC ground-state energies for HF $v=0$ and $v=1$ in Table I, calculated on additive and nonadditive PESs, respectively. The frequency shifts $\Delta\nu_{n,i}$ (5D, ad.) and $\Delta\nu_{n,i}$ (5D, nonad.) are from the quantum 5D calculations (rigid Ar$_n$) for the additive (Ref. 8) and nonadditive (Ref. 10) PESs. The indices m and i are defined in Table I. The experimental shifts $\Delta\nu_{\text{expt.}}$ are from Ref. 12. The isomeric structures are shown in Fig. 1, and in some cases in Ref. 13.

m	n	i	$\Delta\nu_{n,i}$ (5D, ad.)	$\Delta\nu_{n,i}$ (5D, nonad.)	$\Delta\nu_{n,i}$ (DMC, ad.)	$\Delta\nu_{n,i}$ (DMC, nonad.)	$\Delta\nu_{\text{expt.}}$	Figure
1	1	1	−9.66		−9.65±0.08		−9.62	
2	2	1	−15.60	−14.78	−15.51±0.10	−14.45±0.12	−14.82	1(a)
3	3	1	−21.11	−19.25	−20.75±0.13	−18.70±0.12	−19.42	1(b)
3	4	1	−21.72	−19.57	−21.32±0.16	−19.06±0.16	−19.87	1(c)
3	5	1	−22.13		−21.64±0.15	−19.30±0.13	−20.17	1(e)
3	6	3			−21.78±0.21	−19.66±0.18	−20.44[a]	1(i)
3	6	4			−21.67±0.23		−20.44[a]	1(j)
3	7	1			−22.17±0.21	−19.97±0.21	−20.69[a]	1(m)
4	4	2	−24.29	−22.02	−23.40±0.16	−21.42±0.15	−22.15	1(d)
4	5	2	−24.65		−23.99±0.14	−21.70±0.15	−22.50	1(f)
4	6	1	−25.25		−24.53±0.21	−22.10±0.15	−22.80	1(h)
4	7	2			−24.81±0.24	−22.42±0.17	−23.09	1(n)
4	8	1	−25.73		−25.01±0.28			Ref. 13
4	10	3			−25.39±0.37			Ref. 13
5	5	3	−26.65		−25.59±0.16	−23.64±0.17	−24.32	1(g)
5	6	7	−26.17		−25.05±0.23	−23.37±0.25		1(k)
5	6	9			−26.00±0.25	−23.81±0.23	−24.66	1(l)
5	9	2			−26.28±0.33			Ref. 13
5	11	2			−27.18±0.45			Ref. 13
6	6	2	−28.99		−28.54±0.20	−26.11±0.18	−26.9[b]	Ref. 13
6	8	3	−29.86		−29.44±0.23			Ref. 13
6	12	2			−30.54±0.61			Ref. 13
9	9	1	−37.20		−35.65±0.31		−33.4[b]	1(o)
10	10	1	−38.57		−36.81±0.38			Ref. 13
11	11	1			−38.85±0.43			Ref. 13
12	12	1	−42.26	−39.20	−40.67±0.42			1(p)

[a]The assignment is not definitive. For additional discussion, see the text.
[b]Estimated from the plot in Fig. 6 of Ref. 12.

redshifts for the low-energy isomers of Ar$_n$HF, $n=1-12$, on pairwise-additive and nonadditive PESs, which are given in Table III. Besides the HF redshifts from the DMC calculations, Table III also shows the redshifts obtained by us previously using the quantum 5D calculations on pairwise-additive[8] and nonadditive PESs.[10] The experimental results of Nauta and Miller[12] are displayed as well. These data allow us to address several important issues, which are discussed in the following sections.

1. Rigid vs nonrigid Ar$_n$ calculations of the HF vibrational frequency shifts

The contribution which the Ar$_n$ vibrations make to the HF redshift can be deduced by comparing the HF redshifts in Table III from the quantum 5D (rigid Ar$_n$) and DMC calculations on the pairwise-additive PESs. Table III shows that for $n \leqslant 8$ the quantum 5D and DMC redshifts differ by up to 1 cm^{-1} or 0.6%-4.5%, depending on the cluster size and isomeric structure. For $n=9-12$, this difference is a bit larger, 1.55-1.76 cm^{-1}, but still at most 4.8% of the DMC results.

A closer inspection of Table III reveals that the differences between the quantum 5D and DMC results are generally the largest for certain cluster isomers which have all Ar

atoms in the first solvation shell of the HF: the $i=2$ isomer of $n=4$ [Fig. 1(d)], 3.8%, compared to the surface-HF $i=1$ isomer with the C_{3v} geometry [Fig. 1(c)], only 1.9%; the $i=3$ isomer of $n=5$ [Fig. 1(g)], 4.1%; the $i=1$ isomer of $n=9$ −12 [Figs. 1(o) and 1(p), and in I, 3.91% ($n=12$) to 4.78% ($n=10$). This implies that these fully solvated structures are less rigid than the isomers having the HF on a surface site; hence treating the Ar$_n$ subunit of the former as frozen in the quantum 5D calculations introduces a somewhat larger error in the frequency shifts. However, there are exceptions. For the $i=2$ monolayer isomer of $n=6$ [Fig. 1(b) in I], the error is just 1.58%, which means that the Ar$_6$ pentagonal pyramid is quite rigid. Overall, treating the Ar$_n$ microcluster as rigid causes modest errors of less than 5% in the calculated HF redshifts, relative to the full-dimensional DMC results for $n=1-12$, on the same PESs.

It is evident from Table III that the HF redshifts from both the DMC and the quantum 5D calculations on the pairwise-additive PESs are rather uniformly greater in magnitude than the observed redshifts. The DMC redshifts are in better agreement with the experimental values, which is expected since they are essentially numerically exact for the PES employed.
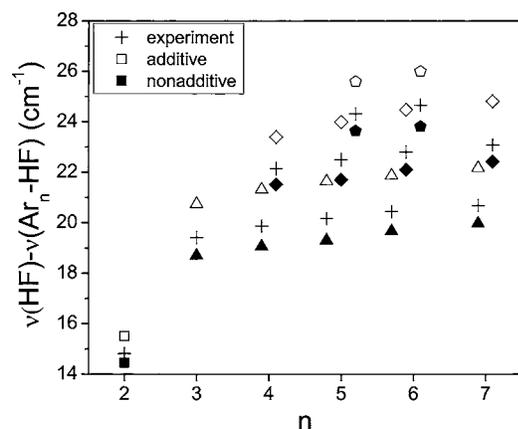
FIG. 2. Comparison of the HF vibrational frequency shifts for $n=2-7$ clusters, from the DMC calculations on additive (empty symbols) and nonadditive potential-energy surfaces (filled symbols), to the experimental data (crosses) from Ref. 12. For $n>3$, the data are shown for two ($n=4,7$) or three ($n=5,6$) lowest-energy isomers of a given cluster size. Triangle, rhombus, and pentagon mark the calculated frequency shifts of the Ar$_n$HF isomers with three, four, and five Ar atoms, respectively, in the first solvent shell of the HF.

2. HF redshifts from DMC calculations on pairwise-additive and nonadditive potential-energy surfaces

Given the very high quality of the Ar–HF and Ar–Ar pair potentials, the residual discrepancies between the DMC redshifts on pairwise-additive PESs and the observed frequency shifts can be attributed principally to the nonadditive interactions. In this section, we discuss mainly the comparison between the HF redshifts from the DMC calculations on pairwise-additive and nonadditive PESs. The pairwise-additive and nonadditive DMC redshifts for the low-lying isomers of the $n=2-7$ clusters are shown in Fig. 2, together with the relevant experimental data.[12]

Figure 2 and Table III show that for the isomers considered, the nonadditive HF redshifts are smaller by $\sim 2-2.5$ cm^{-1} (8%-12%, depending on the cluster size and structure), than their pairwise-additive counterparts. Thus, the contribution of the nonadditive interactions to the vibrational frequency shifts is far from negligible. In fact, for any given cluster isomer, the change in the DMC redshift caused by the inclusion of the nonadditive interactions is about a factor of 2 larger than the difference between the quantum 5D (rigid Ar$_n$) and the DMC redshifts on the same PES.

3. Relationship to experimental results and other theoretical work

It is apparent from Fig. 2 that the nonadditive DMC redshifts agree with the experiment significantly better than the pairwise-additive ones. However, the model of the nonadditivity used here overcorrects the additive results in a remarkably uniform manner: the results on the full nonadditive surfaces typically underestimate the redshifts by 50%–60% of the amount by which the additive surfaces overstimate them. This effect has been seen previously for Ar$_2$HF in Ref. 19, which also found a small but systematic overestimate of the nonadditive shifts in bending frequencies. It may thus be concluded that the "total 1" model of the nonadditivity used here and in Ref. 19 gives a slight overestimate of the overall magnitude of the nonadditive forces but a rather larger overestimate of their dependence on the HF vibrational quantum number.

Although the nonadditive redshifts are all slightly below the experiment, by $0.6-0.8$ cm^{-1}, the theory reproduces extremely well the differences between the HF redshifts measured for the clusters of various sizes and structures. It should be pointed out that the incremental changes in the redshifts from one cluster size and isomer to another were accurately predicted already at the level of the quantum 5D calculations on the pairwise-additive PESs,[7,8] permitting the assignment of the majority of the observed HF frequency shifts.[12] However, these quantum 5D redshifts were consistently larger than the measured values, by $\sim 10\%$.

There are limits on the types of Ar$_n$HF isomers which can be unambiguously identified by means of the HF frequency shift. Those isomers which differ in the number of Ar atoms in the first solvation shell are readily distiguishable by their HF redshifts. On the other hand, when the isomers of a given clusters size have different geometries of the Ar$_n$ subunit but the same number of argons in the first solvent layer around the HF, their respective redshifts are typically a small fraction of a wave number apart, much less than the difference between the measured redshifts and those from the DMC calculations on the pairwise-additive and nonadditive PESs. In these circumstances it is not possible to make a definitive assignment of the measured redshift to one of the cluster isomers.

An example of this is the observed redshift of -20.44 cm^{-1} which was attributed to an isomer of Ar$_6$HF having the HF in a threefold site.[12] The assignment was based on the overall match between the measured and the calculated[8] trends in the frequency shifts; our earlier work, in fact, did not locate any low-lying minima for $n=6$ clusters where the HF was three-coordinated. However, in a subsequent study,[13] we found two very different isomers which have this feature, shown in Figs. 1(i) and 1(j). Their DMC redshifts on the pairwise-additive PESs, -21.78 and -21.67 cm^{-1}, respectively (Table III), differ by only 0.11 cm^{-1}, but are ~ 1.3 cm^{-1} larger in magnitude than the experimental frequency shift, thus precluding its unambiguous assignment.

The same kind of uncertainty exists for the redshift observed at -20.69 cm^{-1} and assigned to an Ar$_7$HF isomer with a three-coordinated HF.[12] Again, the assignment is not unique, since we located three different $n=7$ isomers having this property.[13] The lowest-energy isomer is shown in Fig. 1(m), while the other two are displayed in Fig. 2 in I. The HF frequency shift was calculated using the DMC only for the minimum-energy isomer, but it is clear that the redshifts of the three isomers would be too close to allow positive identification of the isomer responsible for the observed redshift. Achieving reliable assignment in the situations like these for $n=7$ (and $n=6$) would require cluster PESs capable of yielding frequency shifts which are at least an order of magnitude more accurate than the currently available potentials. This is a very difficult challenge for theory.

Two other DMC calculations of the redshifts on Ar_nHF PESs which included nonadditive contributions have been published.[27,28] However, in both of these studies the treatment of the nonadditive interactions was not nearly as rigorous as in the present work, leaving out the nonadditive induction and exchange overlap effects, which have emerged as the dominant nonadditive effects in Ar_2HF.[18] Lewerenz[27] has performed DMC calculations for $n=1-4$ clusters, employing the same pair potentials as we do, but with a much simpler nonadditive potential based on the isotropic Axilrod-Teller interaction, with no vibrational dependence. He found out that the inclusion of such a nonadditive term actually increased the HF redshift, worsening the agreement with the experiment instead of improving it, which indicates deficiencies in his treatment of the nonadditive intermolecular forces. Dykstra's DMC calculations[28] for Ar_nHF clusters used simple model pair potentials of rather low accuracy, and the nonadditive Axilrod-Teller term was used primarily as a means of correcting for the inaccuracy of the pair potentials. The parameters of the Axilrod-Teller term were empirically adjusted to match the experimental redshifts for Ar_2HF and Ar_3HF as well as possible, and then used unchanged in the calculations for larger clusters.

IV. CONCLUSIONS

The work reported in this paper represents the most rigorous and the most comprehensive theoretical study to date of the size and isomer dependence of the HF vibrational frequency shift in Ar_nHF clusters. The diffusion Monte Carlo (DMC) method was employed to calculate the ground-state energies and the HF redshifts on the nonadditive potential-energy surfaces (PESs) for the $n=2-7$ clusters, and on the pairwise-additive PESs for $n=1-12$. This cluster size range includes the closing of the first solvent shell at $n=12$;[6] for $n>3$, the DMC results were obtained for the minimum-energy isomer and for several higher-lying ones energetically closest to it, to enable comparison with the recent experimental data.[12]

On both the pairwise-additive and nonadditive PESs, the energy differences between the DMC ground states of the cluster isomers differ substantially from the energy gaps separating their respective potential minima. This is due to the fact that the intermolecular vibrational zero-point energy (ZPE) varies appreciably from one isomer to another, thus modifying the energy gaps among them. For the clusters with $n=4-8$, the separation of the ground states of the two lowest-lying isomers is much smaller than that between the minima of the potential wells which support the isomers. The situation is reversed for the $n=9-12$ clusters, with the DMC ground-state energy gaps between the isomers being considerably larger than the energy differences between their potential minima. Consequently, identifying the minima, global and local, on the PES is not sufficient for gaining an accurate picture of the relative energetics of the Ar_nHF isomers, which can emerge only from the DMC or other full-dimensional bound-state calculations.

Comparison of the DMC redshifts with those from the quantum 5D calculations,[7,8] mostly on the pairwise-additive PESs (although not exclusively[10]), shows that taking the Ar_n cluster to be rigid in the quantum 5D approach produces results which are only slightly larger, by at most 4.8%, than the corresponding DMC values. Thus, the internal vibrations of the Ar_n subunit play a relatively minor role in determining the size of the HF frequency shift. The DMC results do agree somewhat better in absolute terms with the experimental data. However, the incremental changes (differences) in the redshifts due to variations of the cluster size and isomeric structure are reproduced with comparable accuracy by both the quantum 5D and the DMC calculations on the same PESs.

The DMC redshifts on the nonadditive PESs are ~10% smaller than the frequency shifts calculated using the DMC on the pairwise-additive PESs, and are in considerably better agreement with the experiment. This shows that the nonadditive interactions make a sizable contribution to the HF redshift, and must be taken into account in order for the theory to yield accurate magnitudes of the frequency shifts, not just the incremental redshifts. The nonadditive results are rather uniformly smaller than the experiment by $0.6-0.8$ cm^{-1}, so that an unambiguous assignment is possible in most cases. Difficulties arise in the situations encountered for $n=6, 7$, when several cluster isomers have the same number of argon atoms in the first solvation shell around the HF. Such isomers have very similar HF frequency shifts, and the accuracy of the calculated redshifts is not sufficiently high to identify with certainty the isomer responsible for the observed redshift. Clearly, there is room for further improvements in the description of the nonadditive intermolecular interactions, in particular, their dependence on the intramolecular vibrational excitation of the monomers.

[1] H. S. Gutowsky, T. D. Klots, C. Chuang, C. A. Schmuttenmaer, and T. Emilsson, J. Chem. Phys. **86**, 569 (1987).
[2] H. S. Gutowsky, T. D. Klots, C. Chuang, J. D. Keen, C. A. Schmuttenmaer, and T. Emilsson, J. Am. Chem. Soc. **109**, 5653 (1987).
[3] H. S. Gutowsky, T. D. Klots, C. Chuang, T. Emilsson, R. S. Ruoff, and K. R. Krause, J. Chem. Phys. **88**, 2919 (1988).
[4] A. McIlroy, R. Lascola, C. M. Lovejoy, and D. J. Nesbitt, J. Phys. Chem. **95**, 2636 (1991).
[5] J. T. Farrell, Jr., S. Davis, and D. J. Nesbitt, J. Chem. Phys. **103**, 2395 (1995).
[6] S. Liu, Z. Bačić, J. W. Moskowitz, and K. E. Schmidt, J. Chem. Phys. **100**, 7166 (1994).
[7] S. Liu, Z. Bačić, J. W. Moskowitz, and K. E. Schmidt, J. Chem. Phys. **101**, 10181 (1994).
[8] S. Liu, Z. Bačić, J. W. Moskowitz, and K. E. Schmidt, J. Chem. Phys. **103**, 1829 (1995).
[9] P. Niyaz, Z. Bačić, J. W. Moskowitz, and K. E. Schmidt, Chem. Phys. Lett. **252**, 23 (1996).
[10] J. M. Hutson, S. Liu, J. W. Moskowitz, and Z. Bačić, J. Chem. Phys. **111**, 8378 (1999).
[11] Z. Bačić, J. Chem. Soc., Faraday Trans. **93**, 1459 (1997).
[12] K. Nauta and R. E. Miller, J. Chem. Phys. **115**, 10138 (2001).
[13] M. Xu, H. Jiang, and Z. Bačić, J. Chem. Phys. **121**, 11045 (2004).

[14] R. A. Aziz and H. H. Chen, J. Chem. Phys. **67**, 5719 (1977).

[15] J. M. Hutson, J. Chem. Phys. **96**, 6752 (1992).

[16] A. R. Cooper and J. M. Hutson, J. Chem. Phys. **98**, 5337 (1993).

[17] A. Ernesti and J. M. Hutson, Faraday Discuss. **97**, 119 (1994).

[18] A. Ernesti and J. M. Hutson, Phys. Rev. A **51**, 239 (1995).

[19] A. Ernesti and J. M. Hutson, J. Chem. Phys. **106**, 6288 (1997).

[20] J. B. Anderson, J. Chem. Phys. **63**, 1499 (1975).

[21] J. B. Anderson, J. Chem. Phys. **65**, 4121 (1976).

[22] B. L. Hammond, W. A. Lester, Jr., and P. J. Reynolds. *Monte Carlo Methods in Ab Initio Quantum Chemistry* (World Scientific, Singapore, 1994).

[23] M. A. Suhm and R. O. Watts, Phys. Rep. **204**, 293 (1991).

[24] J. K. Gregory and D. C. Clary, in *Advances in Molecular Vibrations and Collision Dynamics*, edited by J. M. Bowman and Z. Bačić (JAI, Stamford, 1998), Vol. 3, p. 311.

[25] K. B. Whaley, in *Advances in Molecular Vibrations and Collision Dynamics*, edited by J. M. Bowman and Z. Bacvˇić (JAI, Stamford, 1998), Vol. 3., p. 397.

[26] A. Sarsa, K. E. Schmidt, and J. W. Moskowitz, J. Chem. Phys. **113**, 44 (2000).

[27] M. Lewerenz, J. Chem. Phys. **104**, 1028 (1996).

[28] C. E. Dykstra, J. Chem. Phys. **108**, 6619 (1998).